Journal of Physiology (2002), **540.1**, *pp.* 3–14
DOI: 10.1113/jphysiol.2001.013269

www.jphysiol.org

Specific contribution of human T-type calcium channel isotypes (α_{1G}, α_{1H} and α_{1I}) to neuronal excitability

Jean Chemin, Arnaud Monteil, Edward Perez-Reyes *, Emmanuel Bourinet, Joël Nargeot and Philippe Lory

*Institut de Génétique Humaine, CNRS UPR 1142, 141 rue de la Cardonille, F-34396 Montpellier cedex 05, France and * Department of Pharmacology, University of Virgina, 1300 Jefferson Park Avenue, Charlottesville, VA 22908, USA*

In several types of neurons, firing is an intrinsic property produced by specific classes of ion channels. Low-voltage-activated T-type calcium channels (T-channels), which activate with small membrane depolarizations, can generate burst firing and pacemaker activity. Here we have investigated the specific contribution to neuronal excitability of cloned human T-channel subunits. Using HEK-293 cells transiently transfected with the human α_{1G} ($Ca_V3.1$), α_{1H} ($Ca_V3.2$) and α_{1I} ($Ca_V3.3$) subunits, we describe significant differences among these isotypes in their biophysical properties, which are highlighted in action potential clamp studies. Firing activities occurring in cerebellar Purkinje neurons and in thalamocortical relay neurons used as voltage clamp waveforms revealed that α_{1G} channels and, to a lesser extent, α_{1H} channels produced large and transient currents, while currents related to α_{1I} channels exhibited facilitation and produced a sustained calcium entry associated with the depolarizing after-potential interval. Using simulations of reticular and relay thalamic neuron activities, we show that α_{1I} currents contributed to sustained electrical activities, while α_{1G} and α_{1H} currents generated short burst firing. Modelling experiments with the NEURON model further revealed that the α_{1G} channel and α_{1I} channel parameters best accounted for T-channel activities described in thalamocortical relay neurons and in reticular neurons, respectively. Altogether, the data provide evidence for a role of α_{1I} channel in pacemaker activity and further demonstrate that each T-channel pore-forming subunit displays specific gating properties that account for its unique contribution to neuronal firing.

(Received 11 September 2001; accepted after revision 21 December 2001)

Corresponding author P. Lory: Institut de Génétique Humaine (IGH), CNRS UPR 1142, 141, rue de la Cardonille, F-34396 Montpellier cedex 05, France. Email : philippe.lory@igh.cnrs.fr

In the nervous system, information is encoded primarily by the number and the frequency of action potentials. In several types of neurons, firing of action potentials is thought to be an intrinsic property produced by specific ion channels (Llinas, 1988; Connors & Gutnick, 1990). The low-voltage-activated or T-type Ca^{2+} channels (T-channels), a subclass of voltage-gated Ca^{2+} channels, are able to activate from small depolarizations near the resting membrane potential of cells and can generate neuronal spontaneous firing and pacemaker activities (for review see Huguenard, 1996). In rat thalamic relay neurons, T-channels mediate low threshold spikes that are involved in rebound burst firing (Llinas & Jahnsen, 1982). In thalamus, T-channels are involved in slow-wave sleep (Steriade *et al.* 1993; McCormick & Bal, 1997) and in the pathogenesis of epilepsy (Tsakiridou *et al.* 1995; Huguenard, 1999). At this stage, further understanding of the functions and diseased states involving T-channels requires molecular investigations of the channel properties, now made possible by their cloning. Three genes encoding the T-channel pore subunits were identified and designated α_{1G} ($Ca_V3.1$), α_{1H} ($Ca_V3.2$) and α_{1I} ($Ca_V3.3$) (Cribbs *et al.* 1998; Perez-Reyes *et al.* 1998; Klugbauer *et al.* 1999; Lee *et al.* 1999; Williams *et al.* 1999; Monteil *et al.* 2000*a*, 2000*b*; McRory *et al.* 2001). T-currents generated by the α_{1I} subunit display slow kinetics that differ markedly from the α_{1G} and α_{1H} currents which share the typical signature of native neuronal T-currents (Klöckner *et al.* 1999; Monteil *et al.* 2000*b*; McRory *et al.* 2001; for review see Lacinova *et al.* 2000). Northern blot analysis has shown that α_{1G} and α_{1H} mRNA is widely expressed in various tissues and especially in the the central nervous system (CNS) (Cribbs *et al.* 1998; Monteil *et al.* 2000*a*), while the α_{1I} mRNA is restricted to the CNS as well as to thyroid and adrenal glands (Lee *et al.* 1999; Monteil *et al.* 2000*b*). *In situ* hybridization experiments have indicated that the three isotypes can coexist in neuronal tissues such as amygdala or hippocampus, while in the rat cerebellum the α_{1G} subunit is predominant in the same way as α_{1H} in sensory ganglia. In rat thalamus, the α_{1G} and α_{1I} subunits are both present but exhibit distinct expression patterns with respect to the various nuclei (Talley *et al.* 1999). Because Purkinje neurons of the cerebellum and thalamic neurons display intrinsic firing either in short burst or in tonic/sustained mode, we have examined the specific role of T-channel

isotypes in these patterns of activity. Taking advantage of the ability to express pure populations of recombinant T-channels together with the use of voltage clamp protocols mimicking these neuronal activities, we describe here the behaviour of the three human T-channel isotypes in neuronal excitability. These channel properties were modelled to delineate the contribution of each cloned T-channel in promoting firing patterns. This study indicates that the α_{1I} currents are preferentially recruited during the depolarizing after-potential (DAP) and can generate sustained electrical activity, while the α_{1G} and α_{1H} currents promote short burst firing.

METHODS

Cell culture and transfection protocols

Human embryonic kidney cells (HEK-293 cell line; ATCC) were transfected as previously described (Chemin *et al.* 2001) with 0.3 μg of pBB14 plasmid encoding the reporter gene GFP (Brideau *et al.* 1998) and 2.7 μg of different pBK-CMV plasmid constructs that encode for α_{1G} ($\alpha_{1G\text{-}a}$; Chemin *et al.* 2001), α_{1I} (Monteil *et al.* 2000*b*) and α_{1H} (HH7; Cribbs *et al.* 1998). Two to three days later, cells were harvested and plated at low confluence and electrophysiological recordings were performed between days 2 and 6 after transfection.

Electrophysiology

Macroscopic currents were recorded by the whole-cell patch clamp technique using an Axopatch 200B amplifier (Axon Instruments, CA, USA) at room temperature (~25 °C) as previously described (Chemin *et al.* 2001). Extracellular solution contained (mM): 2 $CaCl_2$, 160 TEACl and 10 Hepes (pH adjusted to 7.4 with TEAOH). Borosilicate glass pipettes have a typical resistance of 1–2 MΩ when filled with an internal solution containing (mM): 110 CsCl, 10 EGTA, 10 Hepes, 3 Mg-ATP and 0.6 GTP (pH adjusted to 7.2 with CsOH). For action potential clamp studies we have used: (i) a generic action potential (J. Pancrasio, Axon Instruments website); (ii) a regular train of spikes and a fast burst activity recorded in Purkinje neurons of the cerebellum (Raman & Bean, 1997), generously provided by Dr B. P. Bean (Harvard Medical School, Boston, MA, USA); and (iii) a firing activity typical of those measured on the thalamocortical relay (rTC) neurons generated by the NEURON model (Hines & Carnevale, 1997), described below. Records were filtered at 5 kHz. Cell capacitance was 12.9 ± 2.7 pF (n = 45). Series resistance (R_s) was 14.2 ± 0.6 MΩ (n = 45) and the voltage error factor before compensation was 0.026 ± 0.0016 (n = 45) according to the equation $V_m = V_c(1 - R_s/(R_s + R_m))$, where V_m is the membrane potential, V_c the voltage command and $(R_s/(R_s + R_m))$ the voltage error factor. Capacitance and R_s were compensated by 90–100 % using the whole-cell parameters of the Axopatch 200B amplifier. Leak and residual capacitive currents were subtracted using a P/-5 procedure for tail current recordings and action potential clamp experiments. Data were analysed as previously described (Chemin *et al.* 2001) using pCLAMP6 (Axon Instruments), Excel (Microsoft) and GraphPad Prism (GraphPad Inc.) software. One-way ANOVA combined with a Student-Newman-Keuls *post hoc* test was used to compare the different values, and differences were considered significant at $P < 0.05$. Results are presented as the means ± S.E.M., and n is the number of cells used.

Modelling

The impact of the expression of α_{1G}, α_{1H} and α_{1I} channels on the firing of thalamocortical relay neurons and thalamic reticular neurons was estimated using the NEURON model (described in detail by Hines & Carnevale, 1997). This model was modified by Destexhe *et al.* (1998) for thalamocortical relay cells and by Destexhe *et al.* (1996) for the thalamic reticular neurons. Both models were downloaded from the model database at Yale University (http://senselab.med.yale.edu/senselab/neurondb/). The parameters used in our experiments were the 'three-compartment model configuration of burst behaviour' as described in detail by Destexhe *et al.* (1996). The electrophysiological properties of the α_{1G}, α_{1H} and α_{1I} channels were modelled using Hodgkin-Huxley equations as described by Huguenard & McCormick (1992) and the values obtained for the various α_1 isoforms were substituted for the corresponding values of native T-channels of thalamocortical relay cells (Huguenard & McCormick, 1992) or thalamic reticular neurons (Huguenard & Prince, 1992). All these values are presented in Table 1 except voltage-independent τ of activation, which is 0.8 ± 0.1 (n = 18), 1.34 ± 0.1 (n = 8) and 7.2 ± 0.8 ms (n = 18) for α_{1G}, α_{1H} and α_{1I} channels, respectively. To match the voltage clamp data, the modelling experiments were performed at 28 °C. Firing was triggered by injecting the virtual soma with a 0.18 nA depolarizing current over 100 ms; the resulting activity and the Ca^{2+} entry via T-channels recorded in the soma are presented in Figs 7 and 8. For voltage clamp experiments, a rTC neuronal firing pattern (using native T-channel parameters) was produced by a 0.3 nA current injection into the virtual soma over 700 ms, then converted into a pCLAMP stimulation file and further applied to the transfected HEK-293 cells.

RESULTS

Biophysical properties of the three human cloned T-channels

The T-type Ca^{2+} currents generated by the cloned human α_{1G}, α_{1H} and α_{1I} subunits were studied comparatively in HEK-293 cells. The three subunits produced robust Ca^{2+} currents, as illustrated in Fig. 1*A*. The current–voltage relationships (*I–V* curves) were normalized (Fig. 1*B*), revealing a 7 mV difference in the peak of the *I–V* curve of the α_{1I} current. Steady-state activation curves were deduced from the *I–V* curves (Fig. 1*C*), which were fitted using a combined Boltzmann and linear Ohmic relationships as described previously (Chemin *et al.* 2001). Both steady-state activation and inactivation curves of the α_{1I} current were moved towards positive voltages (7 and 6 mV, respectively), compared to the α_{1G} and α_{1H} currents (Table 1). As a consequence, a ~5 mV positive shift of the window current component of α_{1I} was observed. The three subunits also produced currents that were distinct in their kinetics. Besides the large kinetic differences between the α_{1G} and α_{1I} currents, it is important to note that the α_{1G} subunits generated faster Ca^{2+} currents in both activation and inactivation kinetics compared to the α_{1H} subunit (Fig. 2*A* and *B*, see also Table 1). Furthermore, the major difference between α_{1G} and α_{1H} channels was the recovery from short inactivation, which was significantly slower

(3 times) for the α_{1H} subunit, compared to the α_{1G} subunit (Fig. 2*C* and Table1). A specific electrophysiological feature of T-channels, compared to high-voltage-activated (HVA) Ca^{2+} channels, is their slow deactivation kinetics (Armstrong & Matteson, 1985). Again, significant differences were found among the three human isotypes (Fig. 3*B*), with α_{1I} channels generating the fastest deactivation kinetics as illustrated in Fig. 3*A* while the α_{1H} currents presented the slowest deactivation kinetics (Fig. 3*B* and Table 1). In each case, deactivating tail currents were fitted using a monoexponential function and the rate of deactivation was independent of the current amplitude (not shown), indicating further that accurate voltage control was obtained.

Single action potential clamp studies

Action potential (AP) clamp studies were then performed in order to investigate the specific behaviour of the three T-channel isotypes during neuronal activities. First, we

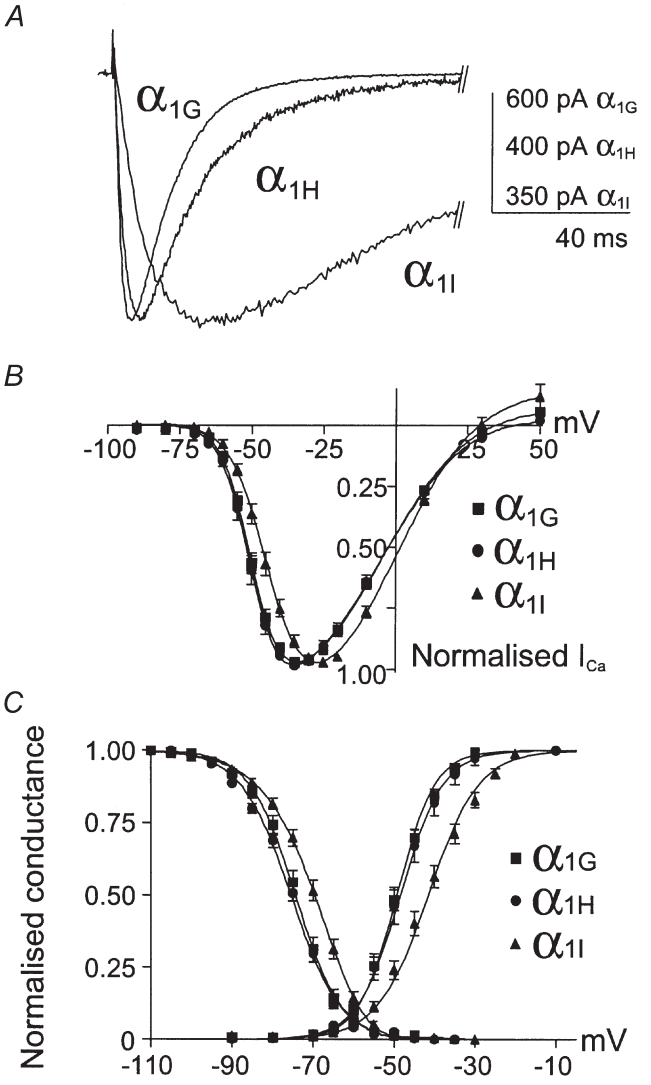

Figure 1

A, typical currents generated by the cloned human α_{1G}, α_{1H} and α_{1I} channels. The traces correspond to the maximal currents elicited by a 100 ms test pulse (TP) from a holding potential (HP) of −110 mV. The voltage values of the TPs are −35 mV for the α_{1G} and α_{1H} subunits and −25 mV for the α_{1I} subunit. *B*, current–voltage relationships (*I–V* curves) for the various α_1 subunits. Note the positive shift of α_{1I} *I–V* curve. *C*, steady-state activation and inactivation curves. Steady-state inactivation curves were obtained by stepping the membrane potential at −30 mV from HPs ranging from −110 to −30 mV. The normalized peak current amplitude was plotted as a function of the HPs.

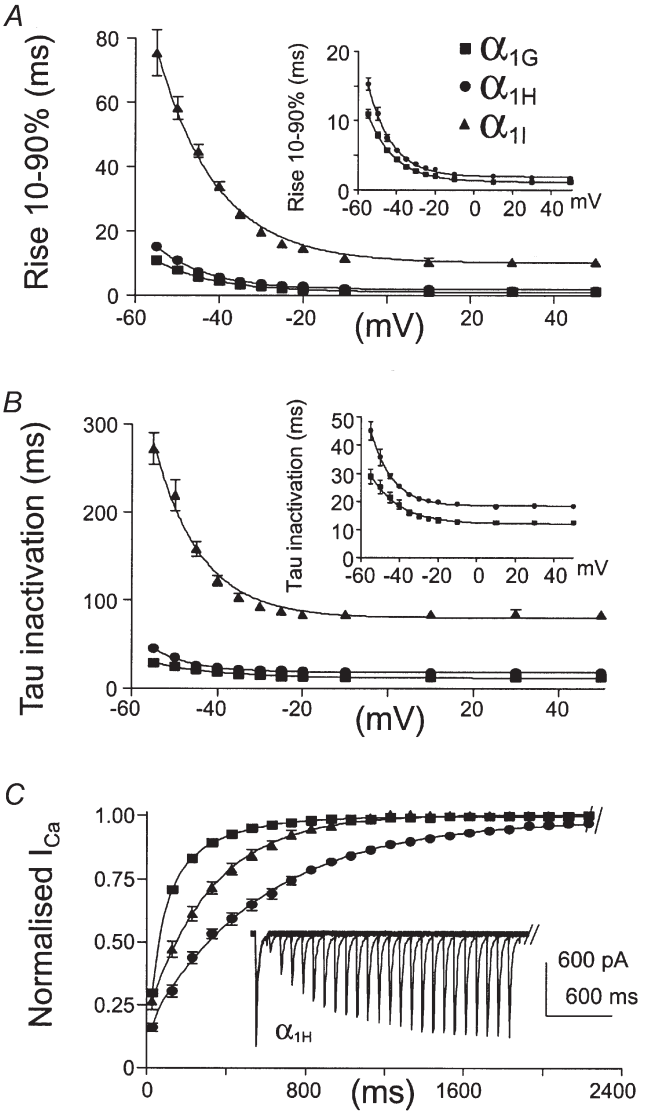

Figure 2

A, activation kinetics were presented as the time for the current to rise from 10 to 90 % (Rise 10–90 %) as function of the test potential. In order to better visualize the difference in activation kinetics between α_{1G} and α_{1H} currents, their corresponding rise times are presented in the inset. *B*, τ of inactivation of the various α_1 isoforms as a function of voltage. Again, τ of inactivation of α_{1G} and α_{1H} currents is presented in the inset. *C*, recovery from short inactivation. As presented for α_{1H} currents, recovery from short inactivation was measured using two −30 mV TPs lasting 100 ms which was applied from a HP of −110 mV of increasing duration.

Table 1. Electrophysiological parameters and statistical comparison of the α_{1G}, α_{1H} and α_{1I} Ca^{2+} currents (2 mM external Ca^{2+}) obtained in HEK-293 cells

	α_{1G}	α_{1H}	α_{1I}	G *vs.* H	G *vs.* I	H *vs.* I
Activation						
$V_{0.5}$ (mV)	−49.3 ± 0.7 (26)	−48.4 ± 1.2 (10)	−41.5 ± 1.1 (17)	n.s.	***	***
Slope (mV)	4.6 ± 0.1 (26)	5.2 ± 0.4 (10)	6.2 ± 0.2 (17)	n.s.	***	*
Inactivation						
$V_{0.5}$ (mV)	−74.2 ± 1.1 (8)	−75.6 ± 0.7 (19)	−69.8 ± 0.9 (17)	n.s.	**	***
Slope (mV)	5.5 ± 0.3 (8)	6.2 ± 0.2 (19)	6.1 ± 0.1 (17)	***	***	n.s.
Activation kinetics						
Rise −40 mV (ms)	4.4 ± 0.2 (20)	5.7 ± 0.2 (9)	33.9 ± 1.4 (31)	*	***	***
Rise +10 mV (ms)	1.2 ± 0.1 (18)	2.1 ± 0.1 (8)	10.5 ± 1.3 (18)	*	***	***
e-fold	14.5 ± 1.2 (17)	11.8 ± 0.8 (9)	14.7 ± 0.8 (29)	n.s.	n.s.	n.s.
Inactivation kinetics						
τ −40 mV (ms)	18.8 ± 1.6 (15)	23.4 ± 0.3 (22)	122 ± 5 (30)	*	***	***
τ +10 mV (ms)	12.6 ± 0.6 (16)	18.2 ± 0.4 (20)	84 ± 3 (32)	*	***	***
e-fold (mV)	10.8 ± 0.9 (16)	6.2 ± 0.6 (11)	9.3 ± 0.6 (26)	**	n.s.	**
Deactivation kinetics						
τ −100 mV (ms)	2.6 ± 0.2 (9)	3.6 ± 0.4 (14)	1.12 ± 0.1 (31)	*	***	***
τ −70 mV (ms)	6.2 ± 0.4 (9)	8.5 ± 1.1 (14)	2.1 ± 0.1 (30)	*	***	***
e-fold (mV)	32.4 ± 2.6 (9)	24.1 ± 1.6 (11)	41 ± 2.6 (30)	n.s.	n.s.	***
τ recovery (ms)	137 ± 5 (12)	448 ± 36 (7)	260 ± 30 (18)	***	**	**

Values are expressed as means ± S.E.M. and *n* is the numbers of cells used. 'Rise', 10–90 % rise time. Statistical comparisons were done using a one-way ANOVA combined with a Student-Newman-Keuls *post hoc* test with * $P < 0.05$, ** $P < 0.01$ and *** $P < 0.001$; n.s., not significant.

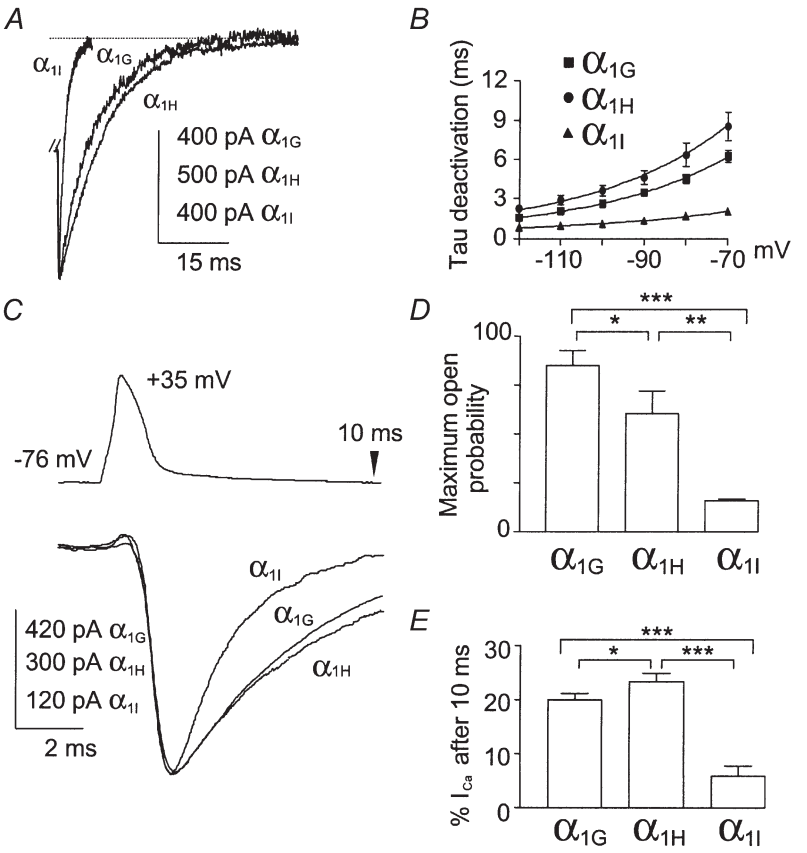

Figure 3

A, and *B*, deactivation kinetics. *A*, examples of normalized deactivating currents at −60 mV elicited after a −30 mV TP from an HP of −110 mV. For each subunit, the TP duration was adapted in order to trigger maximal deactivating currents (4 ms for α_{1G}, 7 ms for α_{1H} and 28 ms for α_{1I} currents). *B*, plot of the deactivation kinetics as a function of the voltage. *C*, *D* and *E*, action potential clamp. *C*, normalized current for the various α_1 isoforms elicited by an action potential (AP). *D*, maximum open probability of the channel isotypes during an AP. Channel maximum open probability during the AP was evaluated by calculating the ratio (*r*) of the maximal current amplitude induced by the AP to the maximal slope conductance (see *I–V* curve; Fig. 1*A*) recorded in the same cell. *E*, histogram of the percentage of the current amplitude remaining 10 ms after the triggering of the AP.

evaluated the contributions of each cloned T-channel during a single AP (Fig. 3*C*). For the three channel isotypes, the onset of Ca^{2+} entry occurred during the repolarization phase of the AP. However, their behaviour during an AP stimulation was markedly distinct. The α_{1I} subunit generated a rapidly inactivating current of small amplitude, revealing that this channel modestly contributed to Ca^{2+} entry during a single AP. In contrast, the α_{1G} and α_{1H} subunits generated larger and sustained currents (Fig. 3*C*). Channel maximum open probability during the AP was evaluated by calculating the ratio (r) of the maximal current amplitude induced by the AP to the maximal slope conductance from the *I–V* curve (see Fig. 1) recorded in the same cell. Maximum open probability (Fig. 3*D*) was larger for the α_{1G} channels ($r = 85.1 \pm 7.4$; $n = 13$) compared to the α_{1H} channels ($r = 60.4 \pm 10.8$; $n = 12$) and to the α_{1I} channels ($r = 16.1 \pm 0.9$; $n = 11$). In order to evaluate the Ca^{2+} entry duration triggered by the AP, we have calculated the percentage of current remaining 10 ms after the beginning of the AP (Fig. 3*E*). The Ca^{2+} entry duration, which reflects deactivation kinetics (Fig. 3*B*), was larger for α_{1G} and α_{1H} channels (percentage of current remaining: 19 ± 1 %, $n = 13$; and 23 ± 1 %, $n = 12$, respectively) compared to α_{1I} channels (6 ± 2 %, $n = 11$). Overall, these data indicated that α_{1G} and α_{1H} channels produce larger and sustained Ca^{2+} entry during a single AP when compared to α_{1I} channels.

Purkinje neuron and thalamocortical relay neuron action potential clamp studies

To further understand the role of the three T-channel isotypes in neuronal excitability, we performed AP clamp studies using several patterns of neuronal activity that occur in Purkinje neurons of the cerebellum (Figs 4 and 5) and in relay neurons of the thalamus (Fig. 6). Although these neuronal activities were recorded in rats, we can predict that our approach is valid since the major T-current properties are conserved among rat and human T-channels (see Klöckner *et al.* 1999). We first applied a typical regular train of spikes (50 Hz) recorded in Purkinje cells (Raman & Bean, 1999*a*) that exhibited sustained spontaneous firing (Fig. 4*A*). In these neurons, APs are generated from a short DAP (18 ms). Several important differences could be observed among the Ca^{2+} currents produced by the three cloned T-channels. The α_{1G} channels rapidly inactivated and only a very small current remained after the tenth spike (Fig. 4*A* and *C*). In contrast, the α_{1I} channels generated a small and transient current during the first interspike interval (~4 times less than the

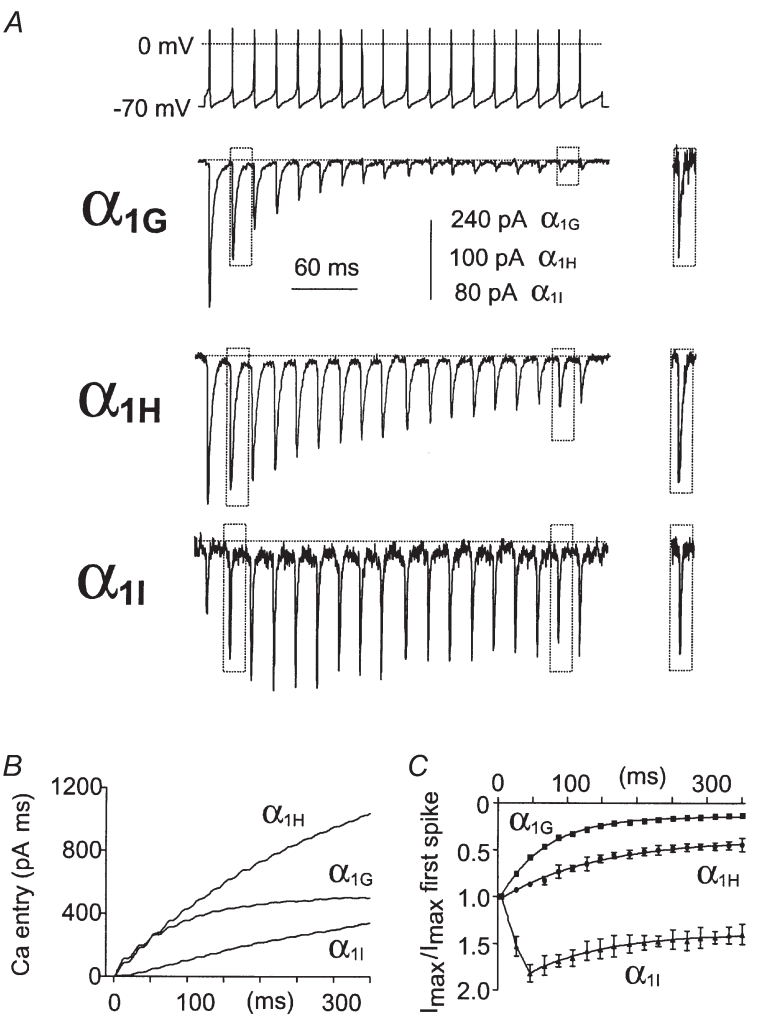

Figure 4. Behaviour of the three T-channel isotypes during tonic firing that occurred in Purkinje neurons

The top trace represents spontaneous activity of a Purkinje neuron which was used to perform AP clamp experiments on transfected cells. *A*, typical recorded currents for the α_{1G}, α_{1H} and α_{1I} channels for cells expressing similar current density for *I–V* curves (see Fig. 1). Expanded and superimposed traces of inward currents triggering from the onset (second) to the end (seventeenth) of AP train stimulation are presented as an inset. *B*, calcium entry as a function of time for the same cells shown in *A*. In order to better compare the calcium entry between α_1 subunits, we normalized it to the maximal slope conductance (from the *I–V* curve; see Fig. 1*A*) recorded in the same cell. *C*, normalized current amplitude for each spike as a function of time.

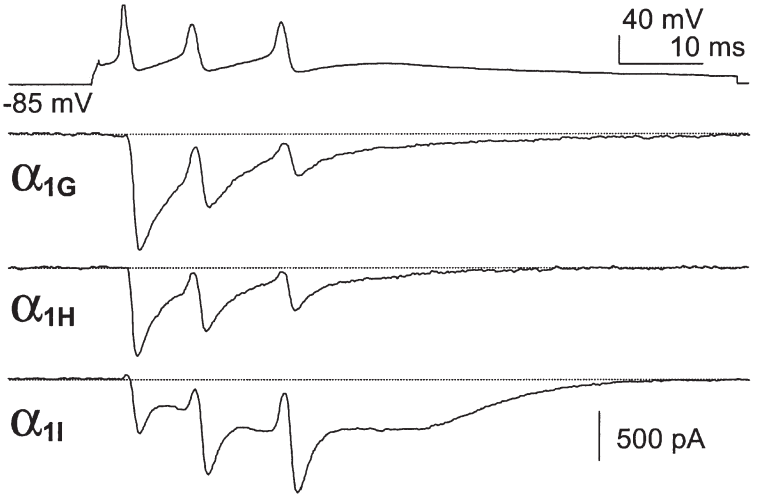

Figure 5. Purkinje neuron burst firing clamp

The top trace represents burst activity of a hyperpolarized Purkinje neuron which was used to perform AP clamp experiments on transfected cells. Typical α_{1G}, α_{1H} and α_{1I} currents for cells expressing similar current density for *I–V* curves. Note the strong facilitation and the large calcium entry during the DAP for α_{1I} currents.

α_{1G} and α_{1H} channels), then increased during the next three spikes (Fig. 4*A* and *C*), suggesting an apparent facilitation of channel activity. After four to five spikes, slow inactivation overcame facilitation leading to a maintained Ca^{2+} entry during the entire train duration (Fig. 4*B* and *C*). The behaviour of the α_{1H} channels was more complex and intermediate between α_{1G} and α_{1I}. The α_{1H} channels contributed to a large depolarizing current during the entire train of stimulation (Fig. 4*A* and *C*) as a consequence of a robust first interspike interval current and slow inactivation, compared to the α_{1G} channels. This difference between α_{1H} and α_{1G} currents was also found using more negative resting potentials. Similar to the result obtained for a holding potential (HP) of –70 mV (Fig. 4*C*), α_{1G} currents decreased more rapidly and the ratio

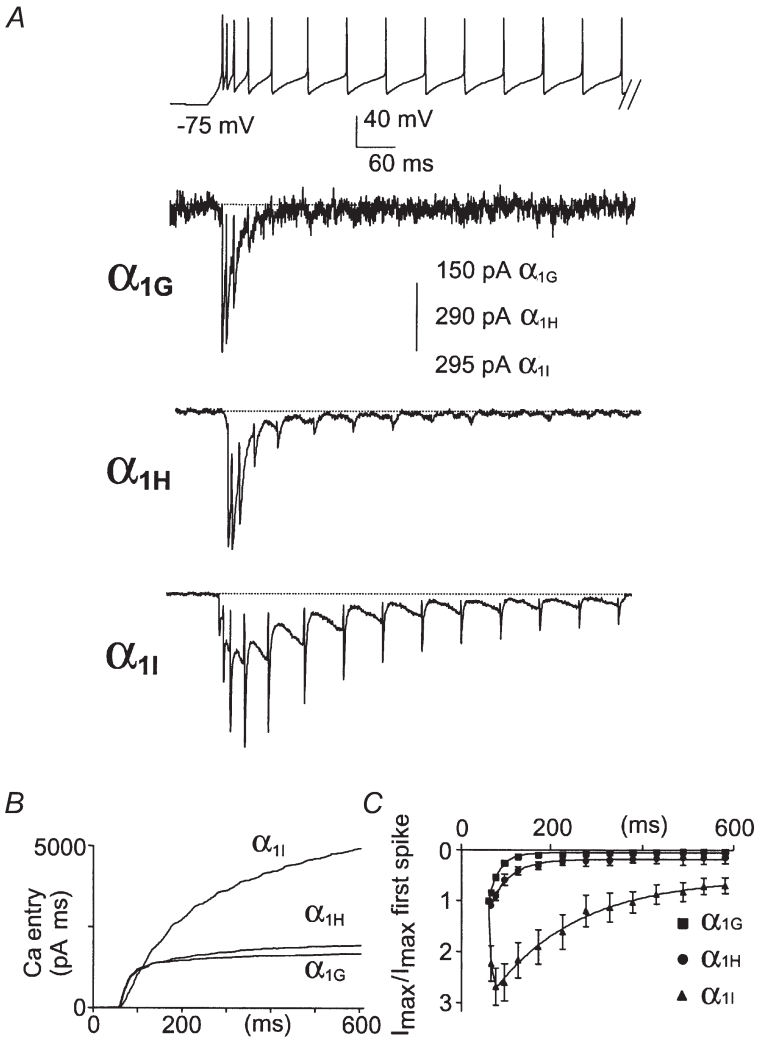

Figure 6. Thalamocortical relay neuron activity clamp

The top trace represents burst activity of a thalamocortical relay neuron which was used to perform AP clamp experiments on transfected cells. *A*, typical α_{1G}, α_{1H} and α_{1I} currents for cells expressing similar current density for *I–V* curves. Note the facilitation and the rebound of the α_{1I} currents during the DAP. *B*, calcium entry as a function of time for the same cells shown in *A*, normalized by the maximal slope conductance from the *I–V* curve (see Fig. 1*A*) recorded in the same cell. *C*, normalized current amplitude for each spike as a function of time.

I_{max} last spike : I_{max} first spike of these currents was ~3 times smaller than the α_{1H} current ratio for a HP of −110 mV ($n = 9$, not shown). Interestingly, the α_{1H} and α_{1I} currents never inactivated completely during the interspike intervals (Fig. 4*A*), leading to a residual Ca^{2+} entry that was still observable at the end of the train of spikes (Fig. 4*B*). The presence of residual current at the steady state suggests that α_{1H} and α_{1I} currents could participate in sustained pacemaker activities. The second and the seventeenth inward current traces were scaled and superimposed (Fig. 4*A*, inset) to further demonstrate an adequate voltage control.

We next performed AP clamp studies using patterns of burst activities. Figure 5 shows the behaviour of the three channel isotypes during short burst activities. When neurons from the Purkinje cell layer of the cerebellum are maintained hyperpolarized, they exhibit short and fast burst s(100 Hz) of a few APs, three on average as used in our experiments, upon injection of a depolarizing current (Raman & Bean, 1997; Fig. 5). In this case, we found that the α_{1G} and α_{1H} channels produced large inward currents that inactivated rapidly (Fig. 5). In contrast, the α_{1I} channels generated a small inward current during the first spike, which strongly facilitated during the next APs. These experiments demonstrated that at a high frequency (100 Hz) the α_{1I} currents still exhibited facilitation. Moreover, it is important to note that an increase of the α_{1I} current amplitude was elicited during the DAP. We then performed voltage clamp analysis using a typical burst firing of the thalamocortical relay (rTC) neurons generated by the NEURON model (Fig. 6; see Methods). The rTC neurons have a resting membrane potential around −75 mV and respond to depolarizations by generating long-lasting burst activities from membrane potentials around −60 mV. As expected from the previous experiments, the α_{1G} and α_{1H} channels generated larger Ca^{2+} entry during the first spikes and then inactivated rapidly (Fig. 6*A* and *B*). No inward currents were observed after about six spikes for either α_{1G} or α_{1H} channels (Fig. 6*C*). In contrast, α_{1I} channels produced large Ca^{2+} entry compared to the α_{1G} and α_{1H} channels (Fig. 6*B*), due to current facilitation and to a large 'rebound' inward current clearly associated with the DAP transition (Fig. 6*A*–*C*). It should be noted, however, that the α_{1H} channels generated a small inward current that occurred during the DAP. Overall, these data suggest that α_{1I}

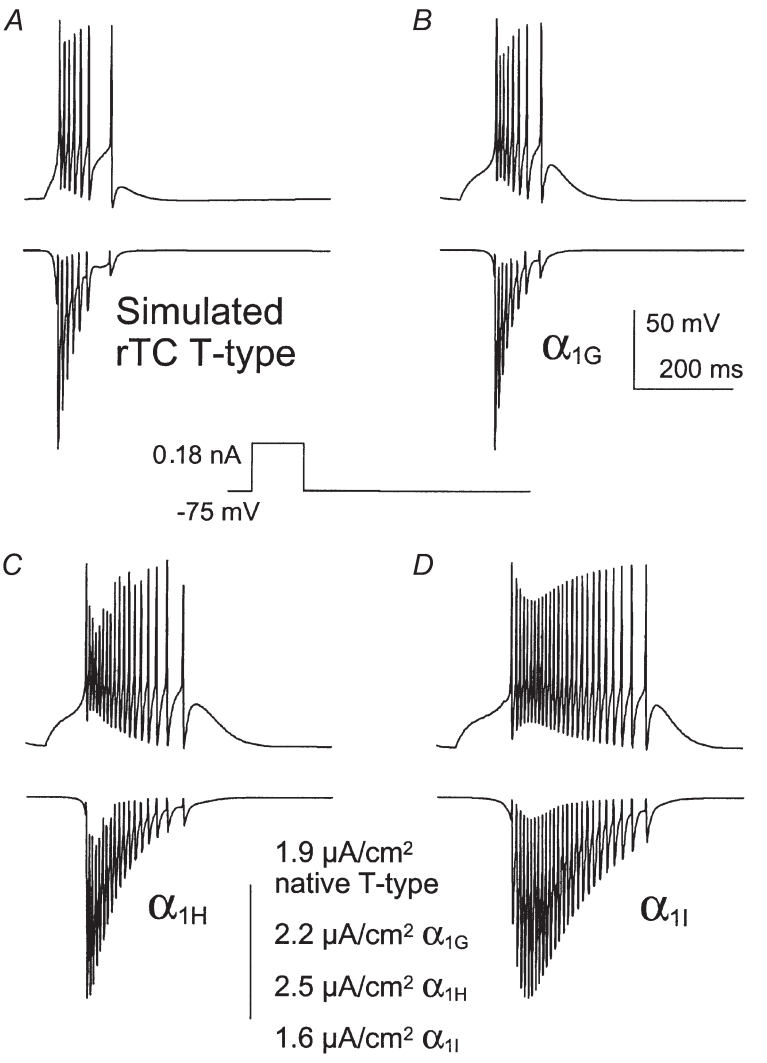

Figure 7. Simulated current clamp recording of thalamocortical relay neurons (rTC)

Cloned T-channel parameters (α_{1G} (*B*), α_{1H} (*C*) and α_{1I} (*D*)) were substituted for the native T-current (*A*) in the model and the resulting firing pattern and calcium entry via T-channels are presented. APs were elicited by a 0.18 nA current injected over 100 ms (see Methods).

currents contribute to sustained neuronal activity, while α_{1G} and α_{1H} current profiles are more consistent with short burst firing.

Modelling experiments

Since action potential clamp studies do not provide dynamic information on the role of T-channels in shaping the neuronal firing patterns, we have performed simulations using the NEURON model (described in detail by Hines & Carnevale, 1997). This model was adapted for thalamocortical relay cells (Fig. 7) and for reticular cells of the thalamus (Fig. 8), as previously described (McCormick & Huguenard, 1992; Destexhe *et al.* 1996, 1998). In each simulation protocol, the parameters describing the native T-current were replaced with those of cloned T-channels. Figure 7*A* shows rTC simulation obtained with the native T-current parameters as described by McCormick & Huguenard (1992). To induce firing, a 100 ms pulse of 180 pA was injected into the virtual soma. This pulse does not trigger APs if T-channels are removed from the model environment (not shown). The parameters of the three cloned T-channels were then sequentially introduced in the model (Fig. 7*B*–*D*). The firing patterns predicted by the α_{1G} channel parameters matched well those produced by the native T-channel parameters of the rTC neurons (Fig. 7*A* and *B*). Both native and α_{1G} currents are able to depolarize the cells to approximately −60 mV during the 100 ms depolarizing pulse, with few APs ($\leqslant 3$) occurring after the stimulation. In addition, these two burst patterns exhibited similar strong frequency adaptation with a rapid decrease in the rate of APs. In both cases, this could be explained by fast current inactivation (see also Fig. 6). The latency to the first spike is nevertheless longer with α_{1G} parameters. This is probably due to the more positive steady-state activation of α_{1G} currents, compared to the native T-currents ($V_{0.5}$ of −49 and −57 mV, respectively). In contrast, firing patterns predicted by α_{1H} and α_{1I} channel activity are markedly different from those

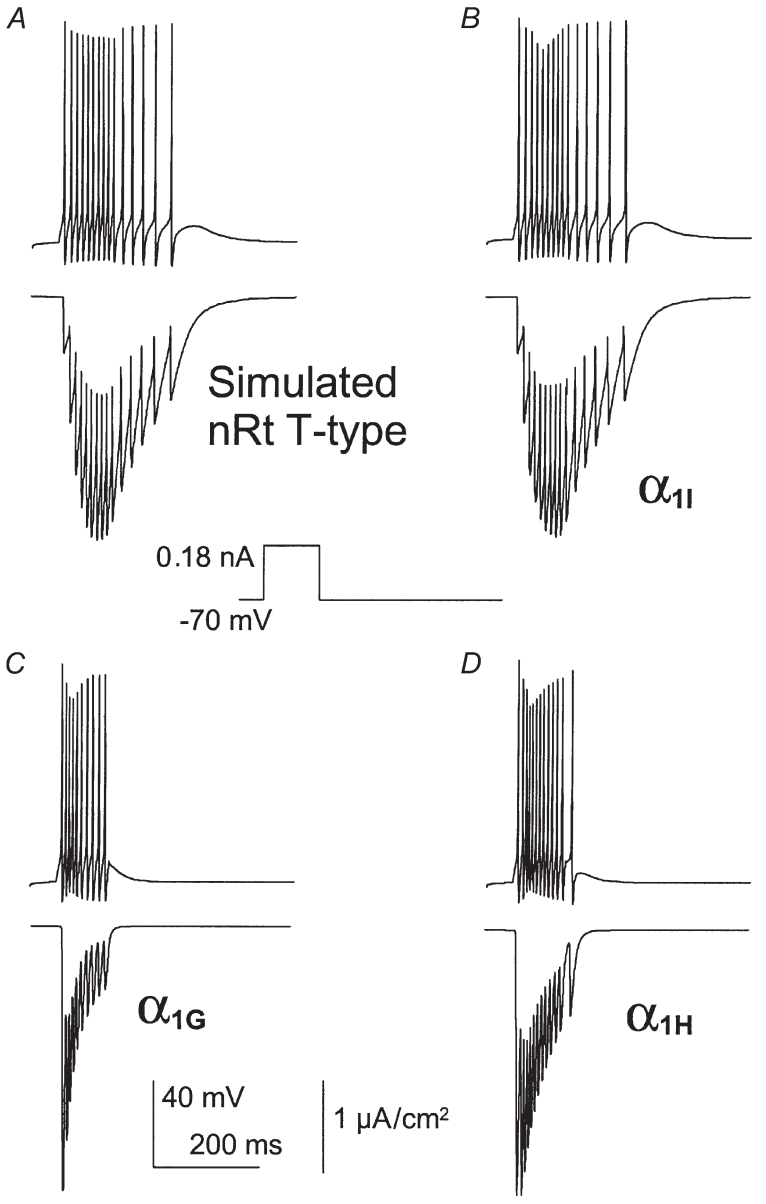

Figure 8. Simulated current clamp recording of the reticular neurons of the thalamus (nRt)

Cloned T-channel parameters (α_{1I} (*B*), α_{1G} (*C*) and α_{1H} (*D*)) were substituted for the native T-current (*A*) in the model and the resulting firing pattern and calcium entry via T-channels are presented. APs were elicited by a 0.18 nA current injected over 100 ms (see Methods).

produced by native T-currents. In both cases, there is a slower frequency adaptation and more importantly, α_{1H} and α_{1I} channels are both able to generate firing even after the end of the stimulation (Fig. 7*C* and *D*). As best exemplified with the α_{1I} parameters, firing continued up to 200 ms after the end of the stimulation. Current facilitation was again observed with the α_{1I} parameters (see also Fig. 6). In addition, the latency to the first AP obtained with the α_{1I} parameters was the longest, probably due to its positive value for $V_{0.5}$ of activation, as well as its slow activation kinetics. Overall, these results are in good agreement with the voltage clamp data described earlier and strongly suggest that the α_{1G} channels are the dominant isotypes functionally expressed in the rTC neurons.

Figure 8 shows T-channel simulations using a thalamic reticular neuron environment. As previously described, firing was induced using a 100 ms pulse of 180 pA injected into the virtual soma. In contrast with thalamocortical relay neurons, firing was predicted to be persistent in reticular neurons (Fig. 8*A*). The α_{1I} parameters best accounted for the firing pattern generated using the native T-current of reticular neurons (Fig. 8*B*; Huguenard & Prince, 1992). Indeed, the native T-current of reticular neurons showed facilitation during the firing activity, as shown for α_{1I} channels both in voltage clamp and modelling experiments. In contrast, the α_{1G} and α_{1H} channels induced firing which stopped at the end of the stimulating pulse (Fig. 8*C* and *D*). Overall, simulation experiments indicated that the α_{1G} and α_{1I} currents might differentially participate in the firing pattern of rTC and reticular neurons of the thalamus and further suggest that α_{1I} channels could promote sustained electrical activities.

DISCUSSION

This study demonstrates that the contribution of T-channels to neuronal excitability is related to isotype-specific properties. The properties of the three human T-channel α_1 subunits cloned to date (α_{1G}, α_{1H} and α_{1I}) were compared and we report significant differences among these isotypes in their biophysical properties, which are highlighted in action potential clamp studies. Modelling experiments further indicate a role of α_{1I} channels in generating pacemaker activity. The functional signatures of the cloned T-channels described here should help both in understanding the diversity of native T-channels and in elucidating their specific physiological roles.

The specific properties of human cloned T-channels

The three T-channel α_1 subunits exhibit distinct functional properties. Compared to α_{1G} and α_{1H} currents, α_{1I} currents show a 6 mV positive shift in their steady-state properties. Because the window current component, a background Ca^{2+} current described in Chemin *et al.* (2000), results from the overlap of the activation and the inactivation curves, the α_{1I} window current component should be evenly shifted. Such a difference could have major consequences on cell phenotype since the window current component of T-channels occurs near physiological resting potential and regulate basal levels of Ca^{2+} (Bijlenga *et al.* 2000; Chemin *et al.* 2000). In thalamocortical neurons, T-window currents contribute to enhanced firing through an intrinsic bistability-mediated phenomenon (Williams *et al.* 1997; Hughes *et al.* 1999). However, there is no evidence to date whether isotype-specific window currents could play distinct roles in neuronal physiology. The three human isotypes also display distinct kinetic properties. Cloned α_{1G} and α_{1H} channels promote fast gated currents typical of native T-currents (Carbone & Lux, 1984; Armstrong & Matteson, 1985; Nowycky *et al.* 1985; Monteil *et al.* 2000*b*), while α_{1I} currents display slow activation and inactivation kinetics but faster deactivation. Nevertheless, α_{1H} currents can be distinguished from α_{1G} currents by their slower activation, inactivation and deactivation kinetics and more importantly by their slow recovery from short inactivation (see also Satin & Cribbs, 2000). These isotype-specific gating properties lead to distinct channel behaviour during neuronal activity. It should be noted, however, that splice variations can tune the properties of each isotype (Chemin *et al.* 2001). Nevertheless, the primary electrophysiological characteristics are isotype specific and conserved among species since the properties of the human cloned T-channels are in good agreement with those obsered in rat counterparts (Klöckner *et al.* 1999).

Activities of cloned T-channels during a single action potential

For T-channels, Ca^{2+} entry occurs mainly during the repolarization phase of the AP. For this reason, the rate of deactivation kinetics is important in tuning the current decay. Due to their slow deactivation kinetics, α_{1G} and α_{1H} channels produce a sustained current typical of that observed in native neurons using similar protocols (McCobb & Beam, 1991; Scroggs & Fox, 1992; Lambert *et al.* 1998). In contrast, the fast deactivation kinetics of α_{1I} channels yields more transient currents during a single AP. Channel maximum open probability during an AP is also related to activation kinetics. Indeed, α_{1I} channels that display slow activation kinetics are not fully activated during a single AP. Similarly, the reduced maximum open probability of α_{1H} channels compared to α_{1G} channels is likely to be due to slower activation kinetics since no significant difference exists in their steady-state properties. In contrast with the data obtained using square test pulses, our results indicate that α_{1G} and α_{1H} channels produce large and sustained Ca^{2+} currents during a single AP, while α_{1I} channels generate small and fast inactivating Ca^{2+} currents. Reciprocally, activation of distinct T-channel populations may differentially influence the shaping of the AP.

Behaviour of cloned T-channels using cerebellum Purkinje neuron activities

The pacemaker activity occurring in Purkinje neurons of the cerebellum is generated by intrinsic properties of these neurons, which abundantly express T-channels (Gruol & Franklin, 1997; Raman & Bean, 1999*a*; Talley *et al.* 1999; Monteil *et al.* 2000*a*; Raman *et al.* 2000). Using neuronal activity of these neurons, we showed that α_{1G} channels produce large and sustained currents during the first interspike intervals that rapidly decrease to a negligible Ca^{2+} entry during prolonged neuronal activity. This fast decrease of the α_{1G} current could be explained by cumulative inactivation resulting from its slow deactivation and its fast inactivation kinetics (Kozlov *et al.* 1999; Serrano *et al.* 1999). The α_{1H} channels are also preferentially recruited during short burst activities but generate persistent current during sustained firing, probably due to their slower inactivation kinetics compared to α_{1G} channels. In contrast, the α_{1I} currents that are tiny and transient during the first interspike interval exhibit apparent facilitation and slow inactivation leading to a sustained Ca^{2+} entry at the steady state. Facilitation that represents cumulative activation, or current summation, could be explained by the slow activation and inactivation kinetics of α_{1I} currents. It is important to note that during fast burst activities, α_{1I} channels generate a large Ca^{2+} current 'rebound' clearly associated with the DAP. Large current associated with the DAP is highly relevant because it probably favours the triggering of the next AP. The rebound of α_{1I} currents during the DAP could be compared to the 'resurgent' sodium current, although it occurs from reopening of previously inactivated sodium channels, that promotes pacemaker activities in Purkinje neurons (Raman & Bean, 1997, 1999*a*,*b*).

Our results suggest that cloned α_{1G} channels are not able to generate pacemaker activities in Purkinje neurons. Similar data were obtained in Purkinje neurons in which native T-current rapidly inactivates during the same train of spikes as used here (Raman & Bean, 1999*a*) suggesting that Purkinje T-currents are generated by α_{1G} channels. Furthermore, these latter authors reported that the block of T-channels by cobalt or mibefradil does not prevent, but only decreases, the firing rate of Purkinje cells. Nevertheless, T-channels could possibly play a role in pacemaker activity after inhibitory synaptic input-induced hyperpolarization of Purkinje neurons (Raman & Bean, 1999*a*). In this case, deinactivated T-channels would generate a large current during the first interspike intervals and participate in the Ca^{2+} entry during short burst activity as observed in our α_{1G} experiments.

Contribution of cloned T-channels to thalamic neuron excitability: action potential clamp and modelling studies

In thalamocortical relay (rTC) and thalamic reticular neurons (nRt), firing activity is proposed to be largely due to the interaction of two currents, the hyperpolarization-activated current, I_h, and the T-current (Jahnsen & Llinas, 1984; McCormick & Pape, 1990). T-current is thought to mediate APs and to control the frequency and time course of repetitive firing. The rTC neurons have a resting potential around −75 mV and respond to depolarization by rhythmic activity generated from a membrane potential around −60 mV (Contreras *et al.* 1993). This phenomenon, called bistability-mediated activity, is related to the T-window current component which maintains the membrane potential near −60 mV (Williams *et al.* 1997; Hughes *et al.* 1999). The voltage clamp data obtained using thalamic activity indicates that α_{1G} and α_{1H} channels produce currents that inactivate rapidly, while α_{1I} currents facilitate and can be recorded during the entire stimulus. It should be noted that sustained α_{1I} current, mainly associated with the DAP, persists even during the slower frequency phase of the burst. These results strongly suggest that α_{1I} current is able to participate and to generate pacemaker activity in thalamic neurons.

The influence of each cloned T-channel on firing patterns was estimated in simulation experiments using the NEURON model adapted for rTC and nRt neurons (McCormick & Huguenard, 1992; Destexhe *et al.* 1996, 1998; Hines & Carnevale, 1997). The modelling experiments are in good agreement with the voltage clamp data. The α_{1G} and α_{1H} currents rapidly inactivate, while α_{1I} currents display facilitation and slowly inactivate during the burst activity. More importantly, modelling experiments demonstrate that α_{1G} currents induce firing activity of short duration while that generated by α_{1I} currents (and to a lesser extent by α_{1H} currents) is significantly more prolonged. Both firing pattern and Ca^{2+} entry induced by simulated α_{1G} currents are similar to those induced by the native T-currents of rTC cells, while α_{1I} currents better account for the native T-currents of nRt neurons. Interestingly, a recent report describing that α_{1I} channels could be modulated by the γ_2 subunit in HEK-293 cells (Green *et al.* 2001) indicates that further studies should investigate the physiological relevance of such a modulation in nRT neurons.

Concluding remarks

The data presented here allow us to ascribe distinct roles in firing activities to each T-channel isotype and complement well the previous observations made for native T-channels in a variety of neurons. Indeed, the critical role of α_{1G} currents in generating burst firing in rTC neurons has just been demonstrated using mice lacking α_{1G} channels (Kim *et al.* 2001). Using neuronal activity as waveforms and modelling studies, we illustrate that α_{1I} channel properties are compatible with a role in sustained neuronal firing and in promoting pacemaker activities. The existence of native T-currents that resemble α_{1I} currents is still a matter of debate. Zhuravleva *et al.* (2001) have reported that 'slow'

and 'fast' components of T-currents can be recorded from thalamic neurons. These data are in good agreement with previous findings from nRt neurons in which slow T-currents participate in the generation of long-duration calcium-dependent spike bursts (Huguenard & Prince, 1992). The behavioural properties of cloned α_{1I} channels described here can account for the T-channel properties in nRt, including long burst firing. Overall, these functional conclusions corroborate well *in situ* hybridization experiments that indicated that the α_{1G} mRNA is predominantly expressed in the rTC nucleus and in cerebellum, while α_{1I} mRNA is strongly expressed in the nRt nucleus, along with α_{1H} mRNA (Talley *et al.* 1999). All together, the finding that T-channel isotypes differentially contribute to neuronal excitability strongly suggests that brain region specific expression of these channels plays an important role in the regulation of information processing in the nervous system.

REFERENCES

Armstrong, C. M. & Matteson, D. R. (1985). Two distinct populations of calcium channels in a clonal line of pituitary cells. *Science* **227**, 65–67.

Bijlenga, P., Liu, J. H., Espinos, E., Haenggeli, C. A., Fischer-Lougheed, J., Bader, C. R. & Bernheim, L. (2000). T-type alpha 1H Ca^{2+} channels are involved in Ca^{2+} signaling during terminal differentiation (fusion) of human myoblasts. *Proceedings of the National Academy of Sciences of the USA* **97**, 7627–7632.

Brideau, A. D., Banfield, B. W. & Enquist, L. W. (1998). The Us9 gene product of pseudorabies virus, an alphaherpes virus, is a phosphorylated, tail-anchored type II membrane protein. *Journal of Virology* **72**, 4560–4570.

Carbone, E. & Lux, H. D. (1984). A low voltage-activated, fully inactivating Ca channel in vertebrate sensory neurones. *Nature* **310**, 501–502.

Chemin, J., Monteil, A., Bourinet, E., Nargeot, J. & Lory, P. (2001). Alternatively spliced alpha1G ($Ca_V3.1$) intracellular loops promote specific T-type Ca^{2+} channel gating properties. *Biophysical Journal* **80**, 1238–1250.

Chemin, J., Monteil, A., Briquaire, C., Richard, S., Perez-Reyes, E., Nargeot, J. & Lory, P. (2000). Overexpression of T-type calcium channels in HEK-293 cells increases intracellular calcium without affecting cellular proliferation. *FEBS Letters* **478**, 166–172.

Connors, B. W. & Gutnick, M. J. (1990). Intrinsic firing patterns of diverse neocortical neurons. *Trends in Neurosciences* **13**, 99–104.

Contreras, D., Curro-Dossi, R. & Steriade, M. (1993). Electrophysiological properties of cat reticular thalamic neurones *in vivo*. *Journal of Physiology* **470**, 273–294.

Cribbs, L. L., Lee, J. H., Yang, J., Satin, J., Zhang, Y., Daud, A., Barclay, J., Williamson, M. P., Fox, M., Rees, M. & Perez-Reyes, E. (1998). Cloning and characterization of alpha1H from human heart, a member of the T-type Ca^{2+} channel gene family. *Circulation Research* **83**, 103–109.

Destexhe, A., Contreras, D., Steriade, M., Sejnowski, T. J. & Huguenard, J. R. (1996). In vivo, in vitro, and computational analysis of dendritic calcium currents in thalamic reticular neurons. *Journal of Neuroscience* **16**, 169–185.

Destexhe, A., Neubig, M., Ulrich, D. & Huguenard, J. (1998). Dendritic low-threshold calcium currents in thalamic relay cells. *Journal of Neuroscience* **18**, 3574–3588.

Green, P. J., Warre, R., Hayes, P. D., McNaughton, N. C. L., Medhurst, A. D., Pangalos, M., Duckworth, D. M. & Randall, A. D. (2001). Kinetic modification of the α_{1I} subunit-mediated T-type Ca^{2+} channel by a human neuronal Ca^{2+} channel γ subunit. *Journal of Physiology* **533**, 467–478.

Gruol, D. L. & Franklin, C. L. (1987). Morphological and physiological differentiation of Purkinje neurons in cultures of rat cerebellum. *Journal of Neuroscience* **7**, 1271–1293.

Hines, M. L. & Carnevale, N. T. (1997). The NEURON simulation environment. *Neural Computation* **9**, 1179–1209.

Hughes, S. W., Cope, D. W., Toth, T. I., Williams, S. R. & Crunelli, V. (1999). All thalamocortical neurones possess a T-type Ca^{2+} 'window' current that enables the expression of bistability-mediated activities. *Journal of Physiology* **517**, 805–815.

Huguenard, J. R. (1996). Low-threshold calcium currents in central nervous system neurons. *Annual Review of Physiology* **58**, 329–348.

Huguenard, J. R. (1999). Neuronal circuitry of thalamocortical epilepsy and mechanisms of antiabsence drug action. *Advances in Neurology* **79**, 991–999.

Huguenard, J. R. & McCormick, D. A. (1992). Simulation of the currents involved in rhythmic oscillations in thalamic relay neurons. *Journal of Neurophysiology* **68**, 1373–1383.

Huguenard, J. R. & Prince, D. A. (1992). A novel T-type current underlies prolonged Ca^{2+}-dependent burst firing in GABAergic neurons of rat thalamic reticular nucleus. *Journal of Neuroscience* **12**, 3804–3817.

Jahnsen, H. & Llinas, R. (1984). Ionic basis for the electro-responsiveness and oscillatory properties of guinea-pig thalamic neurones *in vitro*. *Journal of Physiology* **349**, 227–247.

Kim, D., Song, I., Keum, S., Lee, T., Jeong, M. J., Kim, S. S., McEnery, M. W. & Shi, H. S. (2001). Lack of burst firing of thalamocortical relay neurons and resistance to absence seizures in mice lacking a1G T-type Ca^{2+} channels. *Neuron* **31**, 35–45.

Klöckner, U., Lee, J. H., Cribbs, L. L., Daud, A., Hescheler, J., Pereverzev, A., Perez-Reyes, E. & Schneider, T. (1999). Comparison of the Ca^{2+} currents induced by expression of three cloned alpha1 subunits, alpha1G, alpha1H and alpha1I, of low-voltage-activated T-type Ca^{2+} channels. *European Journal of Neuroscience* **11**, 4171–4178.

Klugbauer, N., Marais, E., Lacinova, L. & Hofmann, F. (1999). A T-type calcium channel from mouse brain. *Pflügers Archiv* **437**, 710–715.

Kozlov, A. S., McKenna, F., Lee, J. H., Cribbs, L. L., Perez-Reyes, E., Feltz, A. & Lambert, R. C. (1999). Distinct kinetics of cloned T-type Ca^{2+} channels lead to differential Ca^{2+} entry and frequency-dependence during mock action potentials. *European Journal of Neuroscience* **11**, 4149–4158.

Lacinova, L., Klugbauer, N. & Hofmann, F. (2000). Low voltage activated calcium channels: from genes to function. *General Physiology and Biophysics* **19**, 121–136.

Lambert, R. C., McKenna, F., Maulet, Y., Talley, E. M., Bayliss, D. A., Cribbs, L. L., Lee, J. H., Perez-Reyes, E. & Feltz, A. (1998). Low-voltage-activated Ca^{2+} currents are generated by members of the CavT subunit family (alpha1G/H) in rat primary sensory neurons. *Journal of Neuroscience* **18**, 8605–8613.

Lee, J. H., Daud, A. N., Cribbs, L. L., Lacerda, A. E., Pereverzev, A., Klöackner, U., Schneider, T. & Perez-Reyes, E. (1999). Cloning and expression of a novel member of the low voltage-activated T-type calcium channel family. *Journal of Neuroscience* **19**, 1912–1921.

Llinas, R. & Jahnsen, H. (1982). Electrophysiology of mammalian thalamic neurones in vitro. *Nature* **297**, 406–408.

Llinas, R. R. (1988). The intrinsic electrophysiological properties of mammalian neurons: insights into central nervous system function. *Science* **242**, 1654–1664.

McCobb, D. P. & Beam, K. G. (1991). Action potential waveform voltage-clamp commands reveal striking differences in calcium entry via low and high voltage-activated calcium channels. *Neuron* **7**, 119–127.

McCormick, D. A. & Bal, T. (1997). Sleep and arousal: thalamocortical mechanisms. *Annual Review of Neuroscience* **20**, 185–215.

McCormick, D. A. & Huguenard, J. R. (1992). A model of the electrophysiological properties of thalamocortical relay neurons. *Journal of Neurophysiology* **68**, 1384–1400.

McCormick, D. A. & Pape, H. C. (1990). Properties of a hyperpolarization-activated cation current and its role in rhythmic oscillation in thalamic relay neurones. *Journal of Physiology* **431**, 291–318.

McRory, J. E., Santi, C. M., Hamming, K. S. C., Mezeyova, J., Sutton, K. G., Baillie, D. L., Stea, A. & Snutch, T. P. (2001). Molecular and functional characterization of a family of rat brain T-type calcium channels. *Journal of Biological Chemistry* **276**, 3999–4011.

Monteil, A., Chemin, J., Bourinet, E., Mennessier, G., Lory, P. & Nargeot, J. (2000*a*). Molecular and functional properties of the human alpha1G subunit that forms T-type calcium channels. *Journal of Biological Chemistry* **275**, 6090–6100.

Monteil, A., Chemin, J., Leuranguer, V., Altier, C., Mennessier, G., Bourinet, E., Lory, P. & Nargeot, J. (2000*b*). Specific properties of T-type calcium channels generated by the human alpha 1I subunit. *Journal of Biological Chemistry* **275**, 16 530–16 535.

Nowycky, M. C., Fox, A. P. & Tsien, R. W. (1985). Three types of neuronal calcium channel with different calcium agonist sensitivity. *Nature* **316**, 440–443.

Perez-Reyes, E., Cribbs, L. L., Daud, A., Lacerda, A. E., Barclay, J., Williamson, M. P., Fox, M., Rees, M. & Lee, J. H. (1998). Molecular characterization of a neuronal low-voltage-activated T-type calcium channel. *Nature* **391**, 896–900.

Raman, I. M. & Bean, B. P. (1997). Resurgent sodium current and action potential formation in dissociated cerebellar Purkinje neurons. *Journal of Neuroscience* **17**, 4517–4126.

Raman, I. M. & Bean, B. P. (1999*a*). Ionic currents underlying spontaneous action potentials in isolated cerebellar Purkinje neurons. *Journal of Neuroscience* **19**, 1663–1674.

Raman, I. M. & Bean, B. P. (1999*b*). Properties of sodium currents and action potential firing in isolated cerebellar Purkinje neurons. *Annals of the New York Academy of Sciences* **868**, 93–96.

Raman, I. M., Gustafson, A. E. & Padgett, D. (2000). Ionic currents and spontaneous firing in neurons isolated from the cerebellar nuclei. *Journal of Neuroscience* **20**, 9004–9016.

Satin, J. & Cribbs, L. L. (2000). Identification of a T-type Ca^{2+} channel isoform in murine atrial myocytes (AT-1 cells). *Circulation Research* **86**, 636–642.

Scroggs, R. S. & Fox, A. P. (1992). Multiple Ca^{2+} currents elicited by action potential waveforms in acutely isolated adult rat dorsal root ganglion neurons. *Journal of Neuroscience* **12**, 1789–1801.

Serrano, J. R., Perez-Reyes, E. & Jones, S. W. (1999). State-dependent inactivation of the alpha1G T-type calcium channel. *Journal of General Physiology* **114**, 185–201.

Steriade, M., McCormick, D. A. & Sejnowski, T. J. (1993). Thalamocortical oscillations in the sleeping and aroused brain. *Science* **262**, 679–685.

Talley, E. M., Cribbs, L. L., Lee, J. H., Daud, A., Perez-Reyes, E. & Bayliss, D. A. (1999). Differential distribution of three members of a gene family encoding low voltage-activated (T-type) calcium channels. *Journal of Neuroscience* **19**, 1895–1911.

Tsakiridou, E., Bertollini, L., deCurtis, M., Avanzini, G. & Pape, H. C. (1995). Selective increase in T-type calcium conductance of reticular thalamic neurons in a rat model of absence epilepsy. *Journal of Neuroscience* **15**, 3110–3117.

Williams, M. E., Washburn, M. S., Hans, M., Urrutia, A., Brust, P. F., Prodanovich, P., Harpold, M. M. & Stauderman, K. A. (1999). Structure and functional characterization of a novel human low-voltage activated calcium channel. *Journal of Neurochemistry* **72**, 791–799.

Williams, S. R., Toth, T. I., Turner, J. P., Hughes, S. W. & Crunelli, V. (1997). The 'window' component of the low threshold Ca^{2+} current produces input signal amplification and bistability in cat and rat thalamocortical neurones. *Journal of Physiology* **505**, 689–705.

Zhuravleva, S. O., Kostyuk, P. G. & Shuba, Y. M. (2001). Subtypes of low voltage-activated Ca^{2+} channels in laterodorsal thalamic neurons: possible localization and physiological roles. *Pflügers Archiv* **441**, 832–839.

Acknowledgements

This work was supported in part by CNRS, the Association pour la Recherche contre le Cancer (ARC), Association Française contre les myopathies (AFM). We thank M. Mangoni, S. Dubel, P. Fontanaud and V. Chevaleyre for helpful discussions and for critical reading of the manuscript and C. Barrére for help with cell cultures.